# Fission-fragment charge yields: Variation of odd-even staggering with element number, energy, and charge asymmetry

Peter Möller,[1,*] Jørgen Randrup,[2] Akira Iwamoto,[3] and Takatoshi Ichikawa[4]
[1]*Theoretical Division, Los Alamos National Laboratory, Los Alamos, New Mexico 87545, USA*
[2]*Nuclear Science Division, Lawrence Berkeley National Laboratory, Berkeley, California 94720, USA*
[3]*Advanced Science Research Center, Japan Atomic Energy Agency (JAEA), Tokai-mura, Naka-gun, Ibaraki 319-1195, Japan*
[4]*Yukawa Institute for Theoretical Physics, Kyoto University, Kyoto 606-8502, Japan*
(Received 29 May 2013; revised manuscript received 10 January 2014; published 10 July 2014)

**Background:** Fission-fragment charge-yield distributions exhibit a pronounced odd-even staggering. For actinide nuclei the staggering decreases with increasing proton number and with increasing excitation energy. In our calculations of fission yields [Phys. Rev. Lett. **106**, 132503 (2011)] we obtained charge-yield distributions for a number of actinide nuclides by means of random walks on tabulated five-dimensional potential-energy surfaces. However, because the potential-energy model treats the system as a single, compound system during all stages of the fission process, in which individual fragment properties do not appear, no odd-even staggering appeared in the calculated yield curves.
**Purpose:** We have recently become aware that in the experimental data displayed in Fig. 1 in the above paper, there is a remarkable similarity in the odd-even staggering in fission of $^{240}$Pu at thermal neutron energy and fission of $^{234}$U in photon-induced fission at around 11 MeV. We discuss how this similarity and how the variation in the magnitude of the odd-even staggering for three Th isotopes with charge asymmetry and isotope can be qualitatively understood based on strongly damped shape evolution on our calculated five-dimensional potential-energy surfaces.
**Methods:** We conduct random walks on our tabulated five-dimensional potential-energy surfaces and study the difference between the total compound-nucleus energy and the potential energy for the different systems from saddle to scission. Under the strong-damping assumption this difference is the internal excitation energy. We also determine this quantity for different charge splits, symmetric and asymmetric.
**Results:** We find that the magnitude of the odd-even staggering in the charge distribution in the several cases studied here correlates well, inversely, with the excitation energy above the potential-energy surface in the postsaddle region.
**Conclusions:** Because the observed magnitude of the odd-even staggering correlates well with excitation energy over the region where the individual character of the fission fragments emerges, the Brownian shape-motion method can be expected to reproduce this feature, provided a potential-energy model is developed that accounts for how the nascent fragment properties are expressed in the calculated potential-energy surfaces.

DOI: 10.1103/PhysRevC.90.014601 PACS number(s): 25.85.Ca, 24.10.Lx, 24.75.+i, 25.85.Jg

## I. INTRODUCTION

Our previous investigations [1–5] have shown that it is possible to obtain an overall good description of the experimentally observed fission-fragment charge distributions for light actinide nuclides by means of random walks on tabulated five-dimensional (5D) potential-energy surfaces. It was particularly encouraging that the location of the transition from symmetric fission for light Th isotopes to asymmetric fission for the heavier isotopes could be reproduced. Although the transition develops somewhat gradually along the isotopic chain, it can be stated that the transition occurs roughly at $^{226}$Th, where the asymmetric and symmetric peaks in the yield curves are about equal in height, see Fig. 1. At its current state of development our method cannot produce any odd-even staggering. The reason is that in the calculation of the potential energy there is no "individual" treatment of the two nascent fragments, rather the pairing equations are solved for the single compound system. However, odd-even staggering is clearly related to pairing in the nascent fragments as their individual character becomes established.

## II. CALCULATIONS

For our further discussion we need to introduce three simple energy concepts. Let us first recall that in the Brownian shape motion (BSM) model, with its strongly damped motion, there is no pre-scission kinetic energy, or collective energy. We therefore only need three energy concepts for our discussion, namely, (1) the potential-energy $U(\text{def})$ which is the energy of the nucleus at the specific deformation, (2) the total energy $E_{\text{tot}}$, which is the energy (mass) of the nucleus in its ground state plus the excitation energy $E^*$ imparted to the nucleus in the experiment, and (3) the excitation energy $E_{\text{ex}}(\text{def})$ above the potential $U(\text{def})$ at the specific deformation discussed. These were four symbols but since $E^* = E_{\text{ex}}(\text{gs})$ is a "shorthand" for the excitation energy at the ground state, there are

*moller@lanl.gov

 

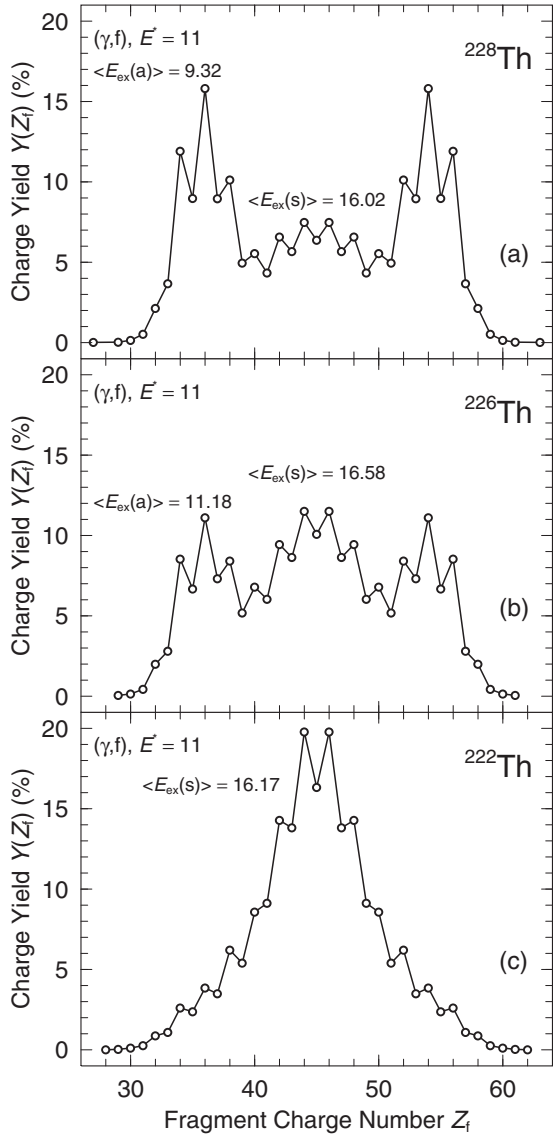


FIG. 1. Measured charge yields in ($\gamma$,f) reactions for $^{228}$Th (a), $^{226}$Th (b), and $^{222}$Th (c), from [6], leading to $E^* \approx$ 8–14 MeV; they include contamination from fission after 1n ($\approx$ 15%) and 2n ($\approx$ 5%) emission. The average excitation energies $\langle E_{ex}(a)\rangle$ and $\langle E_{ex}(s)\rangle$ at the end of the asymmetric and symmetric tracks are also given, see text for definitions.

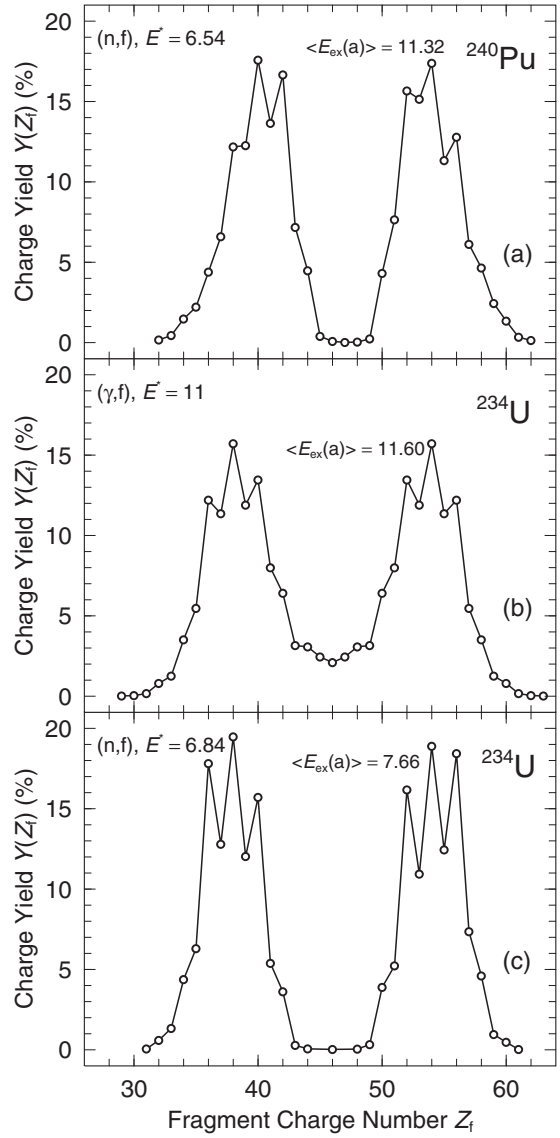


FIG. 2. Measured fission-fragment charge yields. The data in (a) and (c) are for ($n_{th}$,f) reactions leading to $E^* = 6.54$ MeV and $E^* = 6.84$ MeV for $^{240}$Pu and $^{234}$U, respectively, [7] in which some original data are from [8], while the data in (b) are for ($\gamma$,f) reactions leading to $E^* \approx$ 8–14 MeV; they include contamination from fission after 1n ($\approx$ 15%) and 2n ($\approx$ 5%) emission [6]. The average excitation energies $\langle E_{ex}(a)\rangle$ at the end of the asymmetric tracks are also given, see text for definitions.

only three energy concepts. Obviously we have

$$E_{tot} = E_{ex}(\text{def}) + U(\text{def}) = \text{Constant}. \quad (1)$$

Although the BSM model [1] at present cannot quantitatively account for odd-even staggering effects, we can draw some interesting conclusions relating staggering in charge-yield data for Th, U, and Pu to results we obtain in the BSM model. We display some representative experimental charge-yield data in Figs. 1 and 2. We refer to a specific figure panel by (figure number:panel letter) and to table locations by (t:line letter designation). First, let us note that there are only minor differences in the magnitude of the odd-even staggering between $^{233}$U($n_{th}$,f) and $^{235}$U($n_{th}$,f), see (1:c) and (1:b) in [1]. So, in this region, several neutrons away from the transition region, asymmetric fission is well established and a change of the compound-nucleus composition by just one doubly-occupied neutron orbital has relatively little effect on the magnitude of the odd-even staggering. The compound nuclei $^{240}$Pu$^*$ and $^{236}$U$^*$ differ by one neutron orbital and one proton orbital. Because the filling of one neutron orbital made so little difference, one may wonder why the filling of just two orbitals beyond $^{236}$U leads to a much smaller-magnitude odd-even staggering in $^{240}$Pu compared to $^{236}$U.

A possibility that comes to mind is that the observed variation of the odd-even staggering is not a microscopic effect but a macroscopic Coulomb effect. There have been a number of previous discussions of the systematics of odd-even staggering and other fission properties (and the correlations between them) in terms of their variation with respect to various Coulomb-related quantities, such as $Z^2/A$ and $Z^2/A^{1/3}$, referred to as order parameters, see Refs. [8–10] and references therein. But, at this time no fundamental, quantitative model that describes odd-even staggering as a function of compound-nucleus energy and nuclear species has emerged. Here we present some new insights based on treatment in the previously developed BSM model. We emphasize that *no new assumptions or parameters* are introduced.

We show that as the system evolves from saddle to scission the excitation energies above the potential-energy surfaces near scission are very similar in the two systems $\gamma+^{234}$U and $n_{th}+^{239}$Pu leading to compound-nuclei with excitation energies above the *ground states* of approximately 11 MeV and 6.54 MeV, respectively. This again is with the assumption of strongly damped shape motion under which the collective kinetic energy is negligible.

To give an intuitive illustration of our proposed reason behind the similarity between odd-even staggering in the experimental data in Figs. (2:a) and (2:b), we show in Fig. 3 the fission barriers of these compound systems along their asymmetric fission paths. The "one-dimensional" barriers along these "optimal" fission paths are embedded in a 5D deformation space and have been determined as discussed in Refs. [11,12]. The fission potential-energy curves have, as is customary, been expressed relative to the macroscopic energy of the associated spherical nucleus. For $^{234}$U we discuss two excitation energies, 6.84 MeV following thermal neutron absorption on $^{233}$U (2:c) and 11 MeV following $\gamma$ capture (2:b); for $^{240}$Pu we discuss the compound system following thermal-neutron capture leading to 6.54 MeV[1] excitation (2:a). We show in Fig. 3 the total energies of the resulting compound systems as horizontal lines; because the system energy is conserved during fission, the total energy is independent of deformation. To allow straightforward computations of the excitation energy above the potential at the various locations discussed we convert the "compound-nucleus excitation energy" to total energy relative to the spherical macroscopic energy by adding the excitation energy to the ground-state energy given relative to the spherical macroscopic energy. The excitation energy above the barrier at a specific deformation is the internal excitation energy $E_{ex}$ under the assumption of strongly damped motion. It is the difference between the total energy $E_{tot}$ and the barrier potential energy $U$.

At large deformation, specifically $(Q_2/b)^{1/2} = 10$ the excitation energy for $^{234}$U($\gamma$,f) is 11.44 MeV in (3:upper panel), and for $^{240}$Pu($n_{th}$,f) 9.76 MeV in (3:lower panel). Thus, here the excitation energies differ by a modest 1.68 MeV

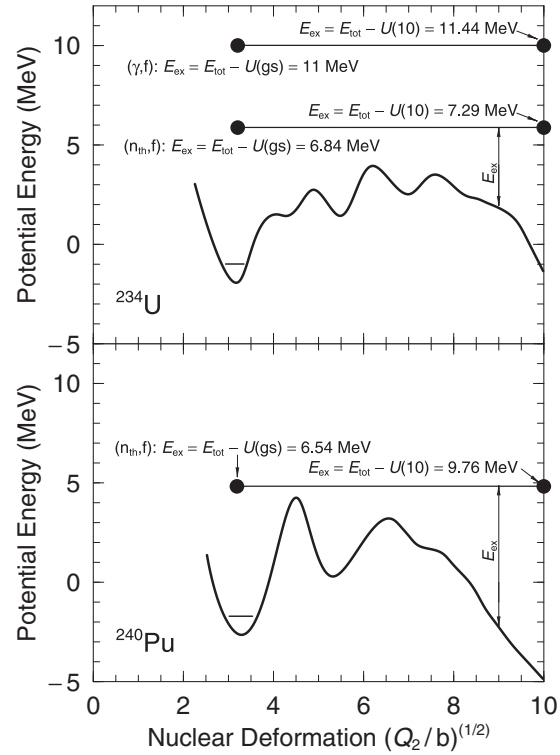


FIG. 3. Calculated potential energy $U$ along the optimum path to scission for $^{234}$U (top panel) and $^{240}$Pu (bottom panel). Plotted for $^{234}$U are the total energies of the compound nuclei following capture of a thermal neutron or an 11-MeV photon (these total energies are conserved during the evolution so they appear as horizontal lines as functions of deformation), while for $^{240}$Pu only the total energy for thermal fission is plotted. Because all energies are given relative to the macroscopic energy of the spherical shape, the excitation energy at a specific deformation is the difference between the total energy and the potential-energy curve, $E_{ex} = E_{tot} - U$. The energies tabulated in Table I are based on ground-state energies that are the sum of the potential energy at the ground-state minimum and a zero-point energy, which is around 0.9 MeV for the nuclei studied here. The ground-state energy has been indicated by a short horizontal line about 0.9 MeV above the potential minimum.

although the compound-nucleus excitation energies differ by 4.46 MeV. This is a plausible reason for the similarity of the odd-even staggering in cases (2:a) and (2:b). In case (2:c) the excitation energy is 7.29 MeV for $^{234}$U in thermal neutron-induced fission, that is 2.47 MeV lower than in (2:a) and 4.15 MeV lower than in (2:b), giving rise to the much larger odd-even staggering observed for (2:c). However, these simple observations are based on the energies at only one single shape.

To make a less arbitrary, more general, quantitative analysis, we show in Table I, in the first three entries, the potential energies of those three systems as the nuclear shape evolves from the ground state towards the shape region where the two nascent fragments have established close to their final properties and the charge asymmetry is roughly frozen in. We also show the corresponding excitation energies above the potential-energy surface. In the six right columns it is the

[1]The excitation energy $E^*$ for thermal-neutron-induced fission, used in [1] in panel (1:a), was 6.84 MeV, but the correct value is 6.54 MeV which we use here. The difference is so small it should have a negligible effect on our current and previous results.

TABLE I. Total energies $E_{\rm tot}$, potential energies $U$, and excitation energies $E_{\rm ex}$ for six different fission reactions at different locations in the 5D deformation space, including three different path endpoints (all, symmetric, and asymmetric). For these latter three locations we calculate values averaged over the track endpoints: the average potential energies $\langle U\rangle$, and the corresponding average excitation energies $\langle E_{\rm ex}\rangle$, by averaging over the endpoints of 10 000 Brownian shape evolutions (All tracks). We also average over "symmetric" tracks only, which we define as those that end with $|\alpha_{\rm g}| \leqslant 0.08$, and over "asymmetric" tracks, which are those with $|\alpha_{\rm g}| > 0.08$, where $\alpha_{\rm g}$ is defined in Eq. (2). All energies are in MeV.

| Case | Reaction | $E_{\rm tot}$ | Ground state | | Saddle | | All tracks | | Sym. tracks | | Asym. tracks | |
|---|---|---|---|---|---|---|---|---|---|---|---|---|
| | | | $U$ | $E^*$ | $U$ | $E_{\rm ex}$ | $\langle U\rangle$ | $\langle E_{\rm ex}\rangle$ | $\langle U(\rm s)\rangle$ | $\langle E_{\rm ex}(\rm s)\rangle$ | $\langle U(\rm a)\rangle$ | $\langle E_{\rm ex}(\rm a)\rangle$ |
| a | $^{239}$Pu(n$_{\rm th}$,f) | 4.86 | −1.68 | 6.54 | 4.20 | 0.66 | −6.40 | 11.26 | −5.89 | 10.75 | −6.46 | 11.32 |
| b | $^{234}$U($\gamma$,f) | 10.05 | −0.95 | 11.00 | 3.95 | 6.10 | −2.10 | 12.15 | −6.27 | 16.32 | −1.55 | 11.60 |
| c | $^{233}$U(n$_{\rm th}$,f) | 5.89 | −0.95 | 6.84 | 3.95 | 1.94 | −1.75 | 7.64 | −1.16 | 7.05 | −1.77 | 7.66 |
| d | $^{228}$Th($\gamma$,f) | 11.00 | 0.00 | 11.00 | 6.46 | 4.54 | 0.74 | 10.26 | −5.02 | 16.02 | 1.68 | 9.32 |
| e | $^{226}$Th($\gamma$,f) | 11.11 | 0.11 | 11.00 | 6.73 | 4.38 | −2.98 | 14.09 | −5.47 | 16.58 | −0.07 | 11.18 |
| f | $^{222}$Th($\gamma$,f) | 9.77 | −1.23 | 11.00 | 6.71 | 3.06 | −5.32 | 15.09 | −6.40 | 16.17 | −2.98 | 12.75 |

average energies at the end of the random-walk tracks that are tabulated. When the shape evolution is highly dissipative, as we are assuming when applying the BSM method, it is this excitation energy that governs to what degree the structure of the potential surface affects the development of structure in the final yield distribution. The local excitation energies above the barriers at the ground states and at the saddles vary considerably between the three reactions considered, but, importantly, the situation is different beyond the saddle region, at elongations where the neck develops and the system acquires a binary character.

To calculate the average excitation energy above the potential-energy surface beyond the saddle in the region where the neck develops, we generate 10 000 BSM trajectories for each of the three cases (2:a), (2:b), and (2:c) and extract the fragment charge distributions from the asymmetry of the shape for which the assumed critical neck radius $c_0 = 2.5$ fm is reached, as discussed in Refs. [1,2]. The energies at the end of the tracks provide the associated distributions of potential energies. The average of these potential energies, $\langle U\rangle$, as well as the corresponding average excitation energies, $\langle E_{\rm ex}\rangle$, are given in Table I for the critical neck radius, $c_0 = 2.5$ fm. We emphasize that our model is not a "scission-point" model. Although we investigate the excitation energies when the critical neck radius is reached, the configuration is governed by the totality of structures in the potential surface from the ground state up to this point. In our treatment the "scission" configurations corresponding to a specific choice of neck radius, such as $c_0 = 2.5$ fm, is a four-dimensional hypersurface consisting of several hundred thousand grid points, embedded in the full five-dimensional potential-energy space [1,3]. When we calculate the endpoint locations of our 10 000 BSM tracks for $c_0 = 2.5$ fm (for the particular sequence of random numbers selected by our algorithm), we reach 5 709 different shape configurations on this surface for $^{234}$U at 11 MeV. As shown in Table I, the average potential energy at these endpoints is −2.10 MeV. The standard deviation of the excitation energy at the track endpoints is 3.09 MeV, but the maximum excitation energy at the end of the tracks is 8.01 MeV and the minimum −13.27 MeV. If we increase the number of tracks to 100 000 we find 21 228 different endpoint configurations, but the average excitation energy changes little, it is now −2.07 MeV.

In our potential-energy calculations we use an asymmetry coordinate $\alpha_{\rm g}$ defined as [12]

$$\alpha_{\rm g} = \frac{Z_{\rm H} - Z_{\rm L}}{Z_{\rm H} + Z_{\rm L}} = \frac{A_{\rm H} - A_{\rm L}}{A_{\rm H} + A_{\rm L}}, \tag{2}$$

where $Z_{\rm H}$ is the charge number of the heavy fragment and $Z_{\rm L}$ that of the light fragment. We have calculated the potential energy for the asymmetry gridpoints $\alpha_{\rm g} = -0.66(0.02)0.66$.

To compare the different endpoint energies of trajectories that terminate in "symmetric" and "asymmetric" configurations, designated (s) and (a) respectively, we define symmetric tracks as those ending with $\alpha_{\rm g} = -0.08(0.02)0.08$ and asymmetric tracks as those outside this interval. For $^{240}$Pu, $\alpha_{\rm g} = 0.08$ corresponds to a charge split $Z_{\rm H} = 50.76$ and $Z_{\rm L} = 43.24$. One should be aware that our calculations use gridpoints related to the asymmetry of the nuclear shape, which when it is converted to particle numbers usually leads to noninteger numbers, since we use the same spacing in $\alpha_{\rm g}$ for all nuclear systems. The experimental data are tabulated for integer values of the charge number $Z$ with a charge-number spacing of 1.

It is apparent that the local excitations in the postsaddle deformation regions where the asymmetries are frozen in are very similar for cases (2:a.t:a) and (2:b,t:b), which both are significantly larger than the corresponding values for case (2:c,t:c). If we limit our discussion to the asymmetric divisions (which are the only ones with significant yield) we find for cases (2:a), (2:b), and (2:c) the excitation energies 11.32 MeV (t:a), 11.60 MeV (t:b), and 7.66 MeV (t:c), respectively. Thus, although the compound excitation energies for $^{234}$U($\gamma$,f) and $^{239}$Pu(n$_{\rm th}$,f) differ by 4.46 MeV, the average local excitations in the postsaddle region differ by only about 0.3 MeV. The much more pronounced odd-even staggering seen in the $^{233}$U(n$_{\rm th}$,f) charge yield can also be qualitatively understood because in this region of the potential-energy surface the average excitation energy over the potential (t:c) is about 4 MeV lower than in the two other reactions (t:a) and (t:b). Therefore the microscopic effects, in particular the pairing effects, in the

potential-energy surface will affect the yield more strongly, leading to a larger-magnitude odd-even staggering.

For the sequence of Th isotopes in Fig. 1 it is also possible to study the variation in odd-even staggering with asymmetry. For $^{226}$Th the magnitudes of the symmetric and asymmetric yields are comparable but the magnitude of the odd-even staggering is different. For $^{226}$Th we find that $\alpha_g = 0.08$ corresponds to a charge split $Z_H = 48.6$ and $Z_L = 41.4$ For this nucleus we find that the average excitation energy at the end of the asymmetric tracks is $\langle E_{ex}(a)\rangle = 11.18$ MeV whereas at the end of the symmetric tracks $\langle E_{ex}(s)\rangle = 16.58$ MeV (t:e), which correlates well with the observed larger-magnitude odd-even staggering in the asymmetric-yield peak compared to the symmetric-yield peak. The different odd-even staggering magnitudes in the asymmetric peak of $^{228}$Th (1:a) and the symmetric peak of $^{222}$Th (1:c) are also well correlated with the average excitation energies at the end of the random-walk tracks; for the symmetric peak of $^{222}$Th we obtain $\langle E_{ex}(s)\rangle = 16.17$ MeV (t:f) and for the asymmetric peak of $^{228}$Th we find $\langle E_{ex}(a)\rangle = 9.32$ MeV (t:d).

## III. SUMMARY

Thus, in summary, we find that the variation of the magnitude of the odd-even staggering in the fission-fragment charge distributions with charge asymmetry and isotope correlates very well (inversely) with the average excitation energy above the potential-energy surface in the region where the neck becomes well developed and the fragments attain their individual character. In contrast, there is little correlation with the excitation energies above the ground-state or saddle regions.

## ACKNOWLEDGMENTS

We are grateful to A. J. Sierk for stimulating discussions and comments. This work was supported by travel grants for P.M. to JUSTIPEN (Japan-U.S. Theory Institute for Physics with Exotic Nuclei) under Grant No. DE-FG02-06ER41407 (U. Tennessee). This work was carried out under the auspices of the National Nuclear Security Administration of the U.S. Department of Energy at Los Alamos National Laboratory under Contract No. DE-AC52-06NA25396. J.R. was supported by the Office of Nuclear Physics in the U.S. Department of Energy's Office of Science under Contract No. DE-AC02-05CH11231. T.I. was supported in part by MEXT SPIRE and JICFuS and JSPS KAKENHI Grant No. 25287065.

[1] J. Randrup and P. Möller, Phys. Rev. Lett. **106**, 132503 (2011).
[2] J. Randrup, P. Möller, and A. J. Sierk, Phys. Rev. C **84**, 034613 (2011).
[3] J. Randrup and P. Möller, in *Proceedings of the 5th International Conference on Fission and Properties of Neutron-Rich Nuclei, Sanibel Island, Florida, 4–10 November 2012* (World Scientific, Singapore, 2013), p. 613.
[4] P. Möller and J. Randrup, in *Proceedings of the 5th International Conference on Fission and Properties of Neutron-Rich Nuclei, Sanibel Island, Florida, 4–10 November 2012* (World Scientific, Singapore, 2013), p. 623.
[5] J. Randrup and P. Möller, Phys. Rev. C **88**, 064606 (2013).
[6] K.-H. Schmidt, S. Steinhäuser, C. Böckstiegel, A. Grewe, A. Heinz, A. R. Junghans, J. Benlliure, H.-G. Clerc, M. de Jong, J. Müller, M. Pfützner, and B. Voss, Nucl. Phys. A **665**, 221 (2000).
[7] M. B. Chadwick, P. Obložinský, M. Herman, N. M. Greene, R. D. McKnight, D. L. Smith, P. G. Young, R. E. MacFarlane, G. M. Hale, R. C. Haight, S. Frankle, A. C. Kahler, T. Kawano, R. C. Little, D. G. Madland, P. Möller, R. Mosteller, P. Page, P. Talou, H. Trellue, M. White, W. B. Wilson, R. Arcilla, C. L. Dunford, S. F. Mughabghab, B. Pritychenko, D. Rochman, A. A. Sonzogni, C. Lubitz, T. H. Trumbull, J. Weinman, D. Brown, D. E. Cullen, D. Heinrichs, D. McNabb, H. Derrien, M. Dunn, N. M. Larson, L. C. Leal, A. D. Carlson, R. C. Block, B. Briggs, E. Cheng, H. Huria, K. Kozier, A. Courcelle, V. Pronyaev, and S. C. van der Marck (CSEWG Collaboration), Nucl. Data Sheets **107**, 2931 (2006).
[8] J. P. Bocquet and R. Brissot, Nucl. Phys. A **502**, 213c (1989).
[9] F. Rejmund, A. V. Ignatyuk, A. R. Junghans, and K.-H. Schmidt, Nucl. Phys. A **678**, 215 (2000).
[10] M. Caamano, F. Rejmund, and K.-H. Schmidt, J. Phys. G: Nucl. Part. Phys. **38**, 035101 (2011).
[11] P. Möller, D. G. Madland, A. J. Sierk, and A. Iwamoto, Nature **409**, 785 (2001).
[12] P. Möller, A. J. Sierk, T. Ichikawa, A. Iwamoto, R. Bengtsson, H. Uhrenholt, and S. Åberg, Phys. Rev. C **79**, 064304 (2009).